Electronic Supplementary Material (ESI) for Journal of Materials Chemistry A.

Supplementary Information

Formamidinium tin-based perovskite with low E_g for photovoltaic applications

Teck Ming Koh,[a,b] *Thirumal Krishnamoorthy,*[b] *Natalia Yantara,*[a,b] *Chen Shi,*[c] *Wei Lin Leong,*[d] *Pablo P. Boix,*[b] *Andrew C. Grimsdale,*[a] *Subodh G. Mhaisalkar*,*[a,b] *Nripan Mathews**[a,b]

[a] School of Materials Science and Engineering, Nanyang Technological University, Singapore, Singapore.
[b] Energy Research Institute @NTU (ERI@N), Singapore, Singapore.
[c] School of Physical and Mathematical Sciences, Nanyang Technological University, Singapore, Singapore.
[d] Institute of Materials Research and Engineering (IMRE), Agency of Science, Technology and Research (A*STAR), Singapore, Singapore.
*Addresses correspondence to: E-mail: Subodh@ntu.edu.sg, Nripan@ntu.edu.sg

EXPERIMENTAL DETAILS

Synthesis of formamidinium iodide [FAI, $HC(NH_2)_2I$]

Briefly, 10 g formamidine acetate salt (Sigma Aldrich, 99%) was dissolved in 10 ml of anhydrous methanol (Sigma-Aldrich, 99.8%) and the solution was cooled in an ice bath. 12.7 ml of hydroiodic acid (Sigma Aldrich, 57 wt % in H_2O) was slowly added into the solution. The solution was allowed to stir for 2 hours and was subsequently dried using rotary evaporator. The precipitate was re-dissolved and recrystallized from diethyl ether (Fisher Scientific, 99.99%). The purification was repeated until white solid was obtained. Yield: 83 %. ^{1}H NMR (400 MHz, DMSO-d_6): δ 8.66 (s, 4H), 7.86 (s, 1H). ^{13}C NMR (400 MHz, DMSO-d_6): δ 158.10.

Device fabrication

The etched Fluorine doped tin oxide (FTO) substrates (Pilkington TEC 15) were cleaned by ultrasonication in decon-soap solution, deionized water and ethanol respectively. A compact layer of TiO_2 was coated onto the FTO substrate by spray pyrolysis process with titanium diisopropoxide bis(acetylacetonate) solution (Sigma-Aldrich, 75% in 2-propanol) diluted with ethanol (Sigma-Aldrich, ≥99.8%) in volume ration of 1:9. After cooling to room temperature, the substrates were treated in a 40 mM $TiCl_4$ solution (Wako Pure Chemical Industries, >99 %) for 30 min at 70 ^{0}C. Mesoporous TiO_2 film was formed by spin-coating DYESOL-30NRD paste (Dyesol, 30 nm TiO_2 nanoparticles), which was diluted with ethanol (Sigma-Aldrich, ≥99.8%) with a ratio of 1:5 w/w, and then sintered at 500 °C for 30 mins. The films were then treated again with 40 mM $TiCl_4$ solution at 70 °C for 30 mins and heated at 500 °C again for 30 mins. $FASnI_3$ film was deposited by spin-coating 1M perovskite solution (dissolving 186 mg of SnI_2, 99.99 % from Sigma-Aldrich, and 86 mg of formamidinium iodide in 500 μL of anhydrous DMF, 99.8 % from Sigma-Aldrich) onto the mesoporous film at 2000 rpm for 40s and then heated at 70 °C for 30 mins. For perovskite solution with SnF_2 addition, 10, 20, 30 and 40 mol % (7.8 mg, 15.7 mg, 23.6 mg and 31.4 mg respectively) of SnF_2 (Sigma-Aldrich, 99%) was added into the 1M $FASnI_3$ solution which has been described above. 2,2',7,7'-tetrakis(*N*,*N*'-di-*p*-methoxyphenylamine)-9,9'-spirobifluorene (spiro-OMeTAD, Merck livilux SHT-263) was prepared in anhydrous chlorobenzene (Sigma-Aldrich, 99.8 %) with a concentration of 100mg/ml. 15.92 µl of *tert*-butylpyridine (96 % from Sigma-Aldrich) and 9.68 µl of lithium bis(trifluoromethylsulfonyl)imide (99.95 % from Sigma-Aldrich, 520mg/ml in acetonitrile) were added directly to the 300 µl of spiro-OMeTAD solution. 3.6 mg of tris(2-(1*H*-pyrazol-1-yl)pyridine)cobalt(III) tris(hexafluorophosphate) Co-dopant (FK102, synthesized according to literature[1]) was pre-dissolved into 13 µl of anhydrous acetonitrile (Sigma-Aldrich, 99.8 %) and added into the hole-transport material solution. The as-prepared spiro-OMeTAD solution was spin-coated onto the perovskite film at 4000 rpm for 30s. A 100 nm Au cathode layer was deposited by thermal evaporation with a 0.2 cm^2 metallic mask. All the fabrication processes and device characterizations were conducted in glove-box.

Reference

1. J. Burschka, A. Dualeh, F. Kessler, E. Baranoff, N. L. Cevey-Ha, C. Y. Yi, M. K. Nazeeruddin and M. Grätzel, J. Am. Chem. Soc., 2011, 133, 18042-18045.

Characterization

^1H and ^{13}C NMR data were obtained on a Bruker DPX 400 MHz spectrometer with chemical shifts referenced to DMSO-d_6. Photovoltaic measurements utilized an AM 1.5G solar simulator equipped with a 450 W xenon lamp (model 81172, Oriel). Its power output was adjusted to match AM 1.5G sunlight (100 mW/cm^2) by using a reference Si photodiode. I−V curves were obtained by applying an external bias to the cell and measuring the generated photocurrent with a

Keithley model 2612A digital source meter. All devices were measured by masking the active area with a black tape mask. Incident-photon-to-current conversion efficiency (IPCE) was measured using a PVE300 (Bentham), with dual Xenon/quartz halogen light source, measured in DC mode and no bias light was used. The absorption spectra were obtained using a UV-Vis spectrometer (SHIMADZU UV-3600 UV-Vis-NIR Spectrophotometer) with an integrated sphere (ISR-3100).

The morphology features and cross-sectional images of devices were observed using a field-emission scanning electron microscope (FE-SEM, JOEL JSM 6700F). XRD patterns of perovskite films were collected using a Bruker D8 Advance diffractometer fitted with a CuK_{α} source operated at 40kV and 40mA, a 1° divergence slit, 0.3mm receiving slit, a secondary graphite monochromator and a Lynxeye silicon strip detector. The XPS and UPS are measured in a home-made UHV system with the base pressure at $3x10^{-10}$ torr. A hemispheric electron analyzer (Omicron, EA125) is used to detect the photoelectron excited by a monochromatic Al Kα radiation (hν=1486.7eV) or UV light (He I, hν=21.2eV). Thermogravimetric analysis (TGA) was conducted using TGA Q500 V6.7 (TA Instruments) with a ramp of 10 ^{o}C/min under nitrogen atmosphere. Differential scanning calorimetry (DSC) was performed on a Q10 V9.9 Build 303 calorimeter (TA Instruments) at a rate of 10 ^{o}C/min under nitrogen.

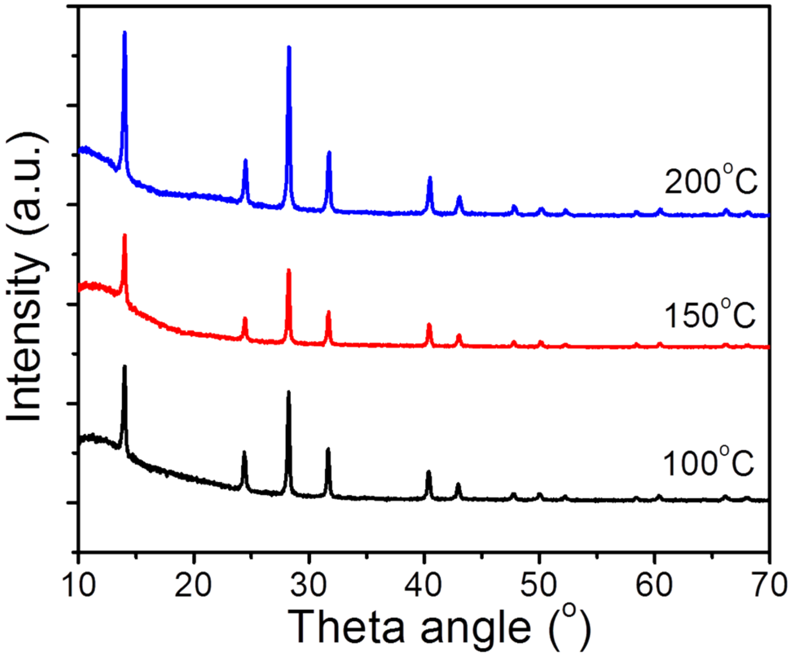

Figure S1. XRD patterns of $FASnI_3$ at different annealing temperatures.

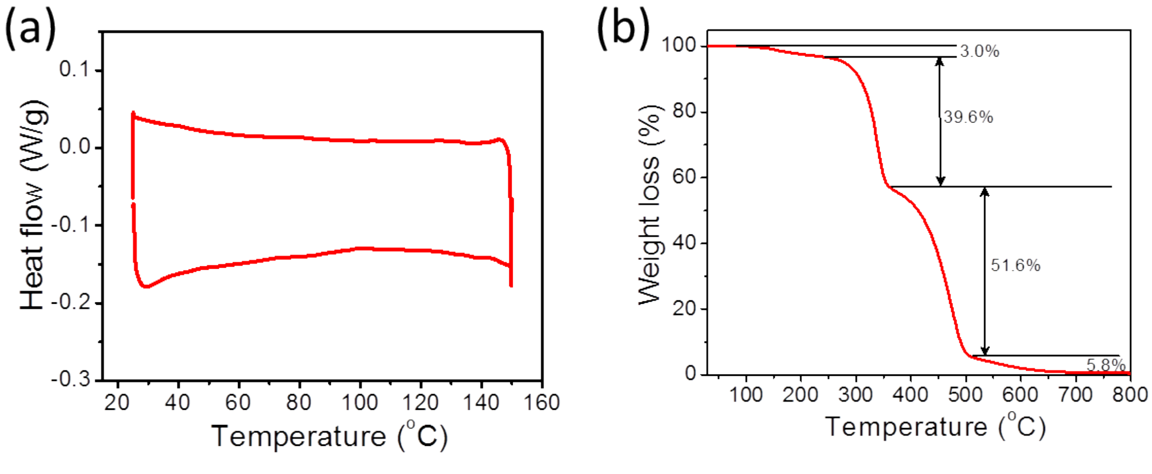

Figure S2. (a) Differential scanning calorimetry (DSC) measurement of $FASnI_3$ The measurement is carried out with heating and cooling rates of ±5 °C/min. (b) TGA curve of $FASnI_3$ powder.

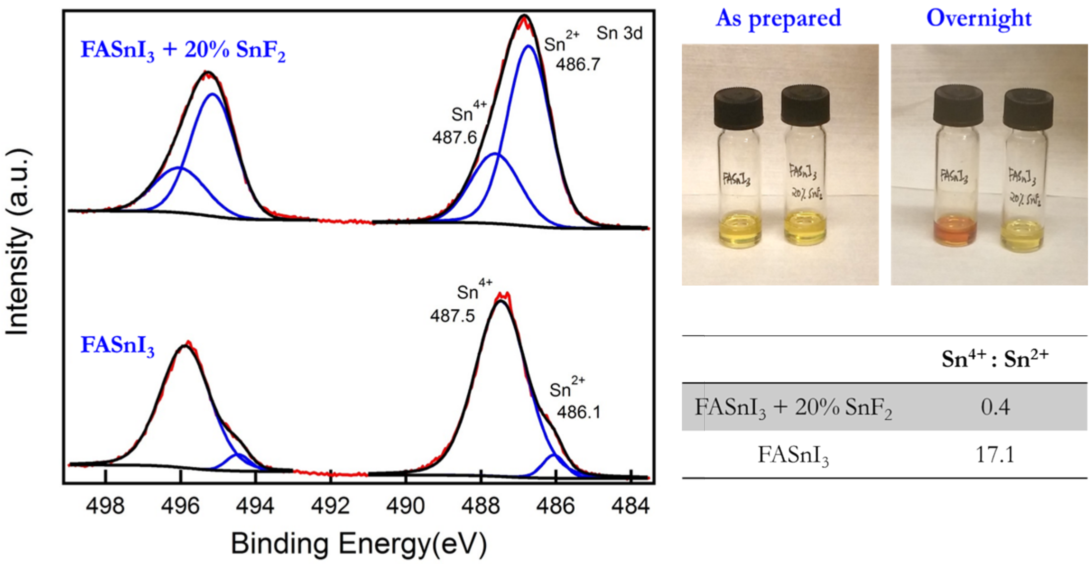

	$Sn^{4+} : Sn^{2+}$
$FASnI_3$ + 20% SnF_2	0.4
$FASnI_3$	17.1

Figure S3. XPS spectra of $FASnI_3$:20%SnF_2 and pure $FASnI_3$ films deposited from solutions stored overnight in gloevbox conditions. The later shows significant arise of Sn^{4+}. Photos indicated the colour change in $FASnI_3$ without SnF_2 addition.

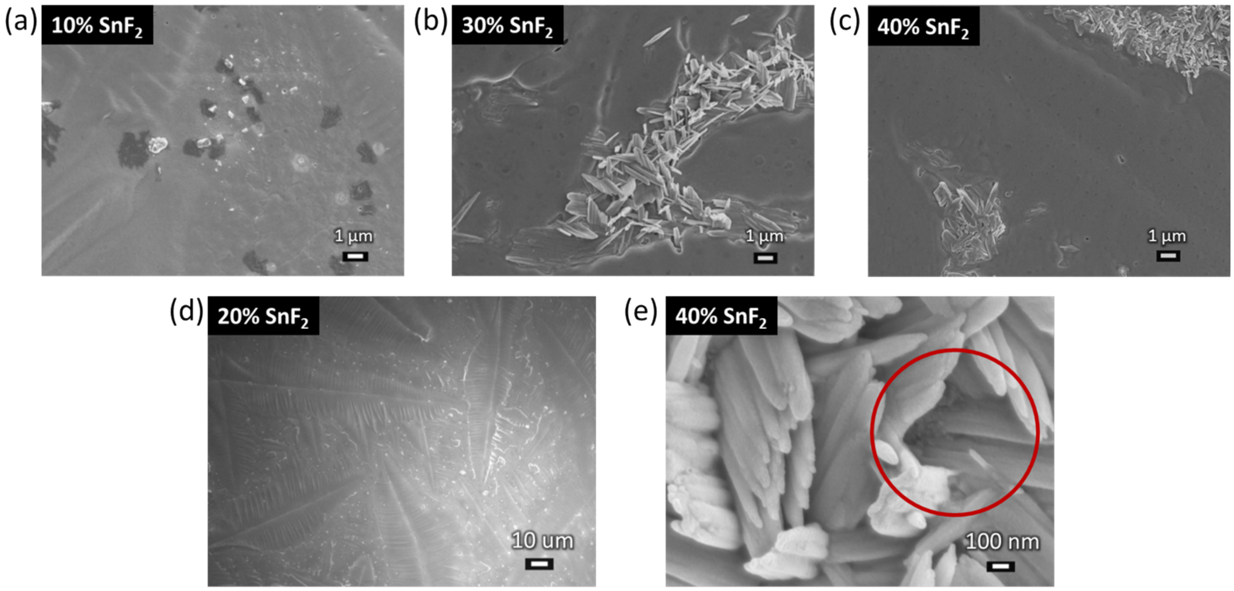

Figure S4. (a-c) Top view FESEM images of $FASnI_3$ perovskite film with different mol% of SnF_2 added, on mesporous TiO_2 layers. (d) FESEM images of surface morphology of $FASnI_3$:20%SnF_2 film on mesoporous TiO_2 layer at low magnification. (e) Bare TiO_2 surface observed at the bottom of the nanoplatelet-like structure is indicated within the red circle.

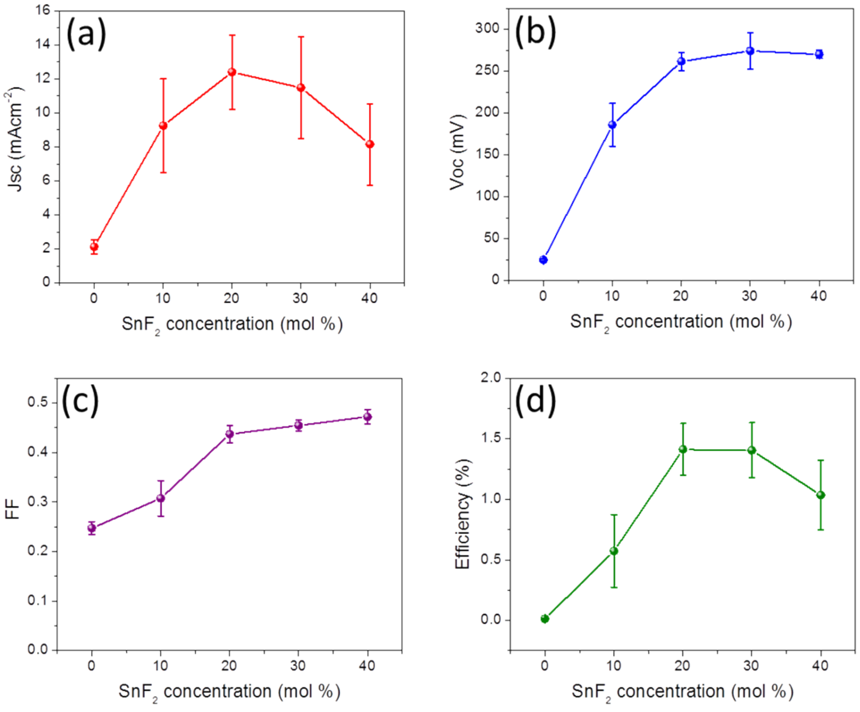

Figure S5. Optimization of addition of SnF_2 into $FASnI_3$. The devices were fabricated on 350 nm mesoporous TiO_2 layers with spiro-OMeTAD as hole conductor.

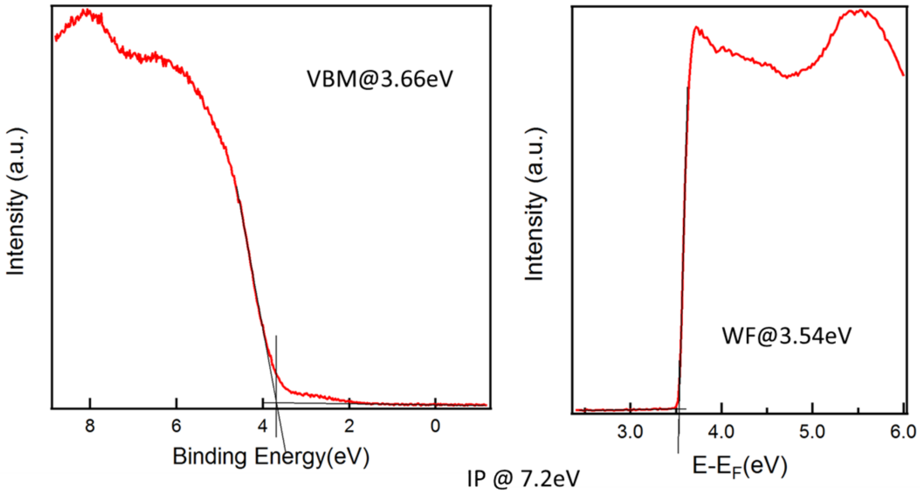

Figure S6. UPS data of nanocrystalline TiO_2.

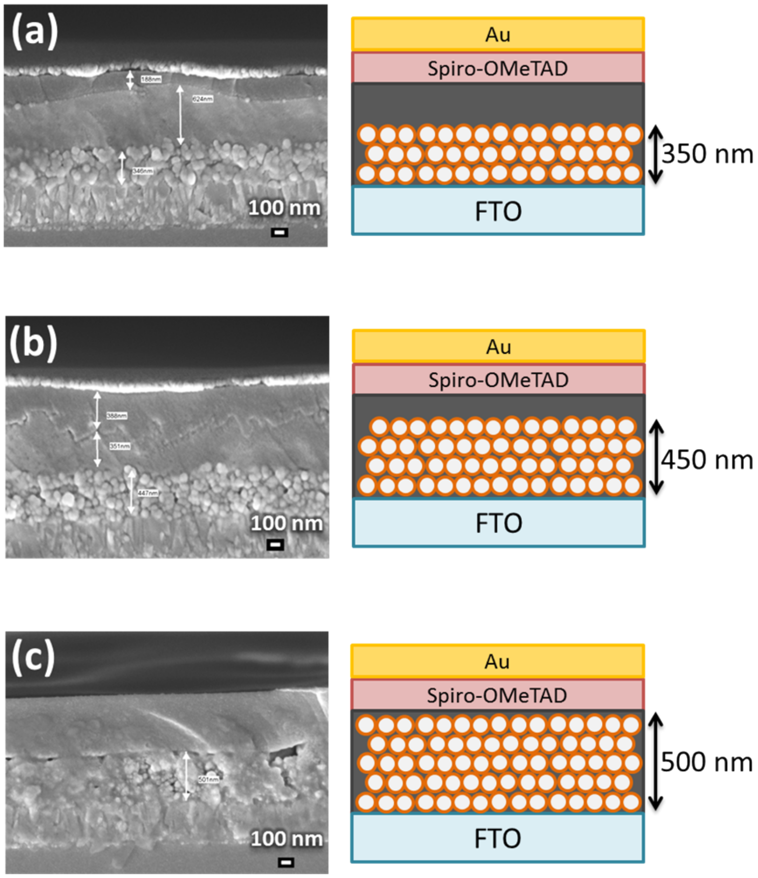

Figure S7. Cross-sectional FESEM images of full device (left) and the schematic structures (right) with different TiO_2 layer thickness.

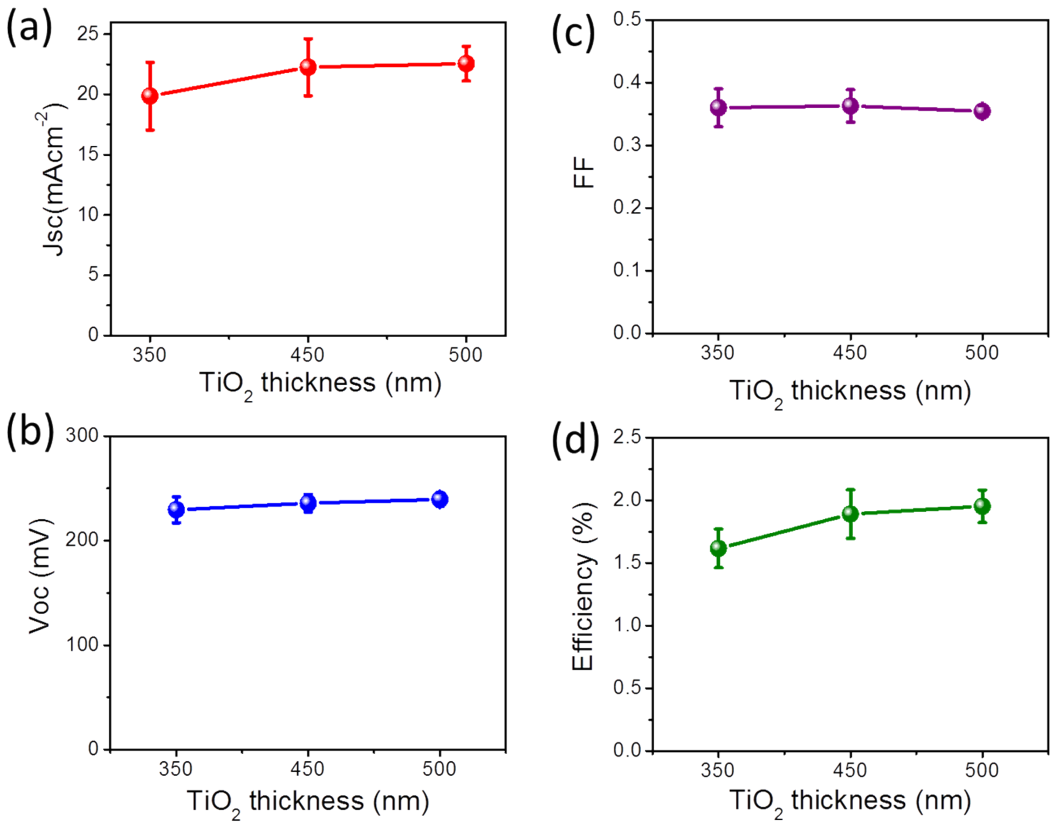

Figure S8. Photovoltaic parameters of devices with different TiO$_2$ thicknesses. 7 devices were fabricated for each thickness.

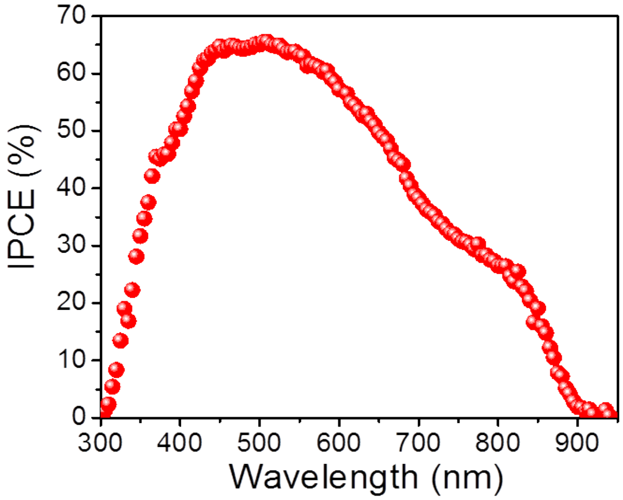

Figure S9. IPCE of FASnI$_3$ deivce with 20 % SnF$_2$ addition.

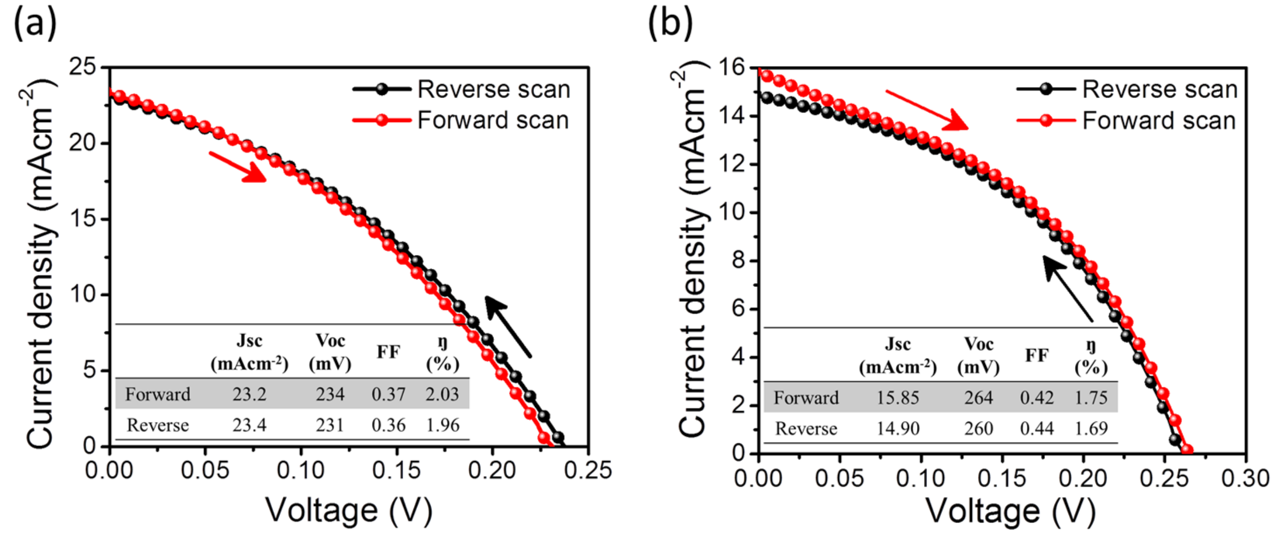

(a)

	Jsc (mAcm^{-2})	Voc (mV)	FF	η (%)
Forward	23.2	234	0.37	2.03
Reverse	23.4	231	0.36	1.96

(b)

	Jsc (mAcm^{-2})	Voc (mV)	FF	η (%)
Forward	15.85	264	0.42	1.75
Reverse	14.90	260	0.44	1.69

Figure S10. *I-V* curves of $FASnI_3$ (20% SnF_2 addition) device using (a) 500 nm and (b) 350 nm mesoporous TiO_2 film in reverse (Voc→Jsc) and forward (Jsc→Voc) scans.